Available online at www.sciencedirect.com

ScienceDirect



Inhibition of the spread of endophytic *Sporisorium reilianum* renders maize resistance to head smut

Xianrong Zhao^{a,b}, Jianrong Ye^a, Lai Wei^a, Nan Zhang^a, Yuexian Xing^c, Weiliang Zuo^a, Qing Chao^{a,d}, Guoqing Tan^c, Mingliang Xu^{a,*}

^aNational Maize Improvement Center of China, China Agricultural University, Beijing 100193, China

^bInstitute of Genetics and Developmental Biology, Chinese Academy of Sciences, Beijing 100101, China

^cMaize Research Institute, Jilin Academy of Agricultural Sciences, Gongzhuling 136100, China

^dInstitute of Botany, Chinese Academy of Sciences, Beijing 100093, China

ARTICLE INFO

Article history:

Received 25 November 2014

Received in revised form

2 February 2015

Accepted 16 February 2015

Available online 21 February 2015

Keywords:

Head smut

Sporisorium reilianum

Maize

Resistance

ABSTRACT

Head smut, caused by the fungal pathogen *Sporisorium reilianum*, poses a grave threat to maize (*Zea mays*) production worldwide. Here we report cytological and molecular evidence for maize resistance to head smut. During early stages of root infection, *S. reilianum* mycelium was capable of penetrating the root epidermis of both resistant (Ji1037) and susceptible (HZ4) inbred lines. *S. reilianum* hyphae were observed in the root–stem junction at 6 days after inoculation. In an attempt to monitor hyphal spread within the maize plant, a highly specific and sensitive real-time PCR method was established to estimate the hyphal content in infected maize tissues. During the upward growth of endophytic *S. reilianum*, the extent of hyphal spread was markedly different between Ji1037 and HZ4. Very little or no pathogen was detected in aerial parts of Ji1037, whereas large amounts of pathogen accumulated in aboveground tissues, particularly inflorescences, of HZ4. Thus, maize resistance to *S. reilianum* was achieved mainly by inhibition of endophytic hyphal growth rather than by prevention of early-root penetration by the pathogen.

© 2015 Crop Science Society of China and Institute of Crop Science, CAAS. Production and hosting by Elsevier B.V. This is an open access article under the CC BY-NC-ND license (<http://creativecommons.org/licenses/by-nc-nd/4.0/>).

1. Introduction

Head smut, caused by *Sporisorium reilianum* f. sp. *zeae* (Kühn) Langdon & Fullerton, is a soilborne systemic fungal disease in maize (*Zea mays* L.) resulting in severe yield losses [1]. Pathogen infection occurs at the seedling stage [2], whereas disease symptoms become apparent at the maturity stage when ear or tassel or both are replaced by large conspicuous galls or sori. Infected plants sometimes exhibit stunted and rosette growth at the vegetative stage, or male sterility,

leading to substantial yield losses. In northern China, the weather conditions and farming systems are conducive to disease development, causing yield losses up to 300,000 tons of grain each year [3].

The causal pathogen *S. reilianum* belongs to the Ustilaginaceae family in the Basidiomycota phylum [2], with a haploid saprophytic and a dikaryotic parasitic life cycle phase [4]. Under favorable conditions, a mature *S. reilianum* teliospore can germinate into a four-celled basidium [5], followed by production of four haploid basidiospores that

* Corresponding author. Tel.: +86 10 62733166.

E-mail address: mxu@cau.edu.cn (M. Xu).

Peer review under responsibility of Crop Science Society of China and Institute of Crop Science, CAAS.

bud to form large numbers of yeastlike spores [6]. The haploid spore cannot infect maize. Only dikaryotic parasitic hyphae derived from the mating of two spores with different mating types are infectious [6]. In soil, the fungus invades host roots without causing appreciable damage to plant tissues [4,7]. *S. reilianum* locally dissolves the epidermal cell wall to penetrate maize roots [4]. Dikaryotic hyphae grow upward as a biotrophic endophyte in the host. The hyphae radically alter the cells when they penetrate floral meristems of susceptible maize, as the fungus switches from biotrophic to necrotrophic growth to begin sporogenesis [7].

S. reilianum has two unlinked mating type loci: *a* and *b* [8]. The *a* locus has three alleles, *a*₁–*a*₃, and encodes a pheromone receptor system responsible for recognition of haploid spores. The *a*₁ allele encodes the pheromones Mfa1.2 and Mfa1.3 and the receptor Pra1. The *a*₂ allele encodes the pheromones Mfa2.1 and Mfa2.3 and the receptor Pra2. The *a*₃ allele encodes the pheromones Mfa3.1 and Mfa3.2 and the receptor Pra3. The homologous pheromone pairs Mfa1.2 and Mfa3.2, Mfa1.3 and Mfa2.3, and Mfa2.1 and Mfa3.1 are detected by receptors Pra2, Pra3, and Pra1, respectively [8]. The *b* locus encodes two regulatory genes, *bE* and *bW*, and has five alleles (*b*₁–*b*₅). The proteins encoded by heterozygous *bE* and *bW* loci can dimerize to form an active transcription factor whose activity is closely associated with the pathogenicity of *S. reilianum* [8].

Detection of plant pathogens is a key step toward the development of effective disease management systems. Conventional methods, which include pathogen isolation and microscopic morphological study, are labor-intensive and cumbersome, sometimes yielding inconclusive results [9]. Rapid, specific, and sensitive molecular tools are required for the detection and evaluation of *S. reilianum*. Xu et al. [10] developed a highly specific and sensitive DNA-based assay for the detection of *S. reilianum* and its differentiation from *Ustilago maydis*, which causes common smut, showing symptoms very similar to those of head smut. Using this method, Tan et al. [11] identified pathogen-carrying plants, and Ni et al. [12] surveyed the rates of plant infection by head smut. In 2012, a method using Fourier transform infrared spectrometry was established for identification of *S. reilianum* spores [13].

The most economical and sustainable means for controlling the disease is the development of resistant varieties, a process that depends on our knowledge of the resistance mechanism. Resistance to head smut is a complex quantitative trait that is under polygenic inheritance. Quantitative trait locus (QTL) analyses have located one major consensus QTL for resistance on chromosome 2, in addition to minor QTL identified on all other chromosomes except for chromosome 7 [1,14]. The major QTL, *qHSR1*, increases head smut resistance in maize by 25%, and this QTL has been further fine-mapped to a 152-kb region [15,16]. Introgression of *qHSR1* into 10 susceptible maize inbred lines via marker-assisted backcrossing (MABC) led to substantial improvement in resistance to head smut [17].

The development of *S. reilianum* sori on maize was investigated by microscopy [18]. The fungus was found mostly in intracellular spaces, suggesting that it passes through the host cell wall by lysis and mechanical pressure [19]. Martinez et al. [4] described the initial infection of maize roots by soilborne *S. reilianum* and later described the saprophytic and parasitic phases of fungal development [7]. Based on

morphological and transcriptional alterations in host plants, Ghareeb et al. [20] proposed a model describing the architectural changes in infected inflorescences as a consequence of transcriptional, hormonal, and redox modulation. Investigating the transcriptional changes in maize infected by head smut, Zhang et al. [3,21] found that the expression patterns of pathogenesis-related genes in HZ4 and Mo17 were differentially regulated at the eighth-leaf stage. Resistance in Mo17 depended on auxin and the regulation of flavonoids in the floral primordium during the early floral transition stage.

Studies of the interaction between *S. reilianum* and the host have focused mostly on pathogen growth in susceptible maize in attempts to discover how *S. reilianum* infects the host [4,7,18–20]. In the present study, we aimed to provide cytological and molecular evidence underlying maize resistance to head smut by comparing the responses of the resistant line Ji1037 and the susceptible line HZ4 during pathogen invasion and hyphal spread.

2. Materials and methods

2.1. Isolation of single-spore colonies of *S. reilianum*

Fresh sori-filled ears were collected from the field and husks were peeled off in a laminar flow cabinet. *S. reilianum* teliospores were suspended in 15 mL potato dextrose broth (PDB) medium (3.5% [w/v] potato dextrose, 0.1 mg mL⁻¹ Amp), and cultured in darkness at 24 °C with 220 r min⁻¹ shaking for 3 days. A 200- μ L aliquot of the culture was streaked on a solid potato dextrose agar (PDA) medium (3.5% [w/v] potato dextrose, 1.5% [w/v] agar, 0.1 mg mL⁻¹ Amp) and incubated in darkness at 28 °C for 3 days. A total of 20 colonies were then isolated from the culture and grown individually in 3.5% PDB medium on a rotary shaker at 220 r min⁻¹ at 24 °C for 3 days. A 10- μ L aliquot was removed from each culture for assessment of purity with a microscope. A 2-mL aliquot from each culture was centrifuged at 12,000 r min⁻¹ for 10 min to collect cell pellets for DNA isolation as described by [22]. DNA of each colony was tested by conventional PCR as described previously [10], using a *S. reilianum*-specific SR1 primer pair (forward: 5'-CAGGTTATGTATGGGCCG-3'; reverse: 5'-TTGAGCGATGACCATTCC-3'), which was tested for specificity for several related pathogens to confirm exclusive amplification of *S. reilianum* and not others, including *U. maydis*. The resulting PCR products from each colony were cloned into the pGEM-T vector and three positive clones from each amplicon were sequenced to minimize possible mismatch nucleotides. The correct sequence of each colony was obtained by multiple sequence alignments among the three sequenced clones using CLUSTALX [23], followed by comparison with the *S. reilianum* genomic sequence deposited in the NCBI database to verify its identity.

2.2. Determination of mating-types for isolated *S. reilianum* colonies

To test the mating type of each colony, several mating type-specific primers were developed. All sequences in the *a* and *b* loci were downloaded from NCBI to design mating-type-specific

markers using Primer3 (<http://frodo.wi.mit.edu/>). Dominant markers mfa1232, mfa1323, and mfa2131 were developed based on the shared sequences of Mfa1.2/Mfa3.2, Mfa1.3/Mfa2.3, and Mfa2.1/Mfa3.1, respectively. Accordingly, *S. reilianum* colonies that showed the PCR band combinations (i) mfa1232 and mfa1323, (ii) mfa2131 and mfa1323, or (iii) mfa2131 and mfa1232, presumably carried the *a1*, *a2*, or *a3* alleles, respectively. For the *b* locus, the dominant markers bw1–bw5, which were designed based on the specific sequences of *bW* in *b1*–*b5*, were used to identify the genotype at the *b* locus for each *S. reilianum* colony. All mating-type-specific markers were used to amplify colonies by conventional PCR.

The conventional PCR reaction mixture contained 1 μL template DNA, 0.2 μL of each primer (0.01 nmol μL^{-1}), 0.2 μL dNTPs (2.5 mmol L^{-1} each), 1 μL 10 \times PCR buffer, 0.1 μL *Taq* DNA polymerase (5 U μL^{-1}) and 7.3 μL double-distilled water (ddH_2O) in a total volume of 10 μL . The PCR program consisted of an initial denaturation step at 94 °C for 3 min, followed by 35 cycles of 30 s at 94 °C, 30 s at 60 °C, and 1 min at 72 °C and was terminated with a final extension step for 10 min at 72 °C. The amplified product was electrophoretically separated on a 2% agarose gel in 1 \times TAE buffer.

After the mating type was identified, the positive colonies were used to inoculate PDA slant culture medium and were incubated at 28 °C for 3 days in darkness and then maintained at 4 °C.

2.3. Plant materials

A highly resistant inbred line Ji1037, derived from the backcross population Mo17//Mo17/Suwan, and a highly susceptible inbred line HZ4, a local inbred line in China, were used. These inbred lines had been grown for many years at the experimental farm of the Jilin Academy of Agricultural Sciences. Under artificial inoculation, the average disease incidence was estimated to be 0 for Ji1037 and 50–80% for HZ4.

2.4. Artificial inoculation with *S. reilianum*

A total of 300 kernels from each inbred line were immersed in distilled water for 10 h, with one replacement with fresh water at 5 h. The kernels were sterilized in 70% ethanol for 1 min, rinsed with distilled water three times, sterilized again in an aqueous solution of 2% (*w/v*) sodium hypochlorite (with Tween 20 at a final concentration of 0.2%) for 30 min with gentle shaking every 10 min, and then washed again with sterilized water three times. Finally, the kernels were soaked in 10% (*w/v*) carbendazim for 12 h and washed in distilled water five times. All of the above treatments were performed at room temperature.

Batches of 14 kernels each were oriented with the embryo facing upward on a piece of wet filter paper placed on the bottom of a sterilized seed germination box (13 cm \times 19 cm \times 12 cm). The box was kept in an incubator at 28 °C with 16-h day/8-h night, 60% relative humidity, and seed watering every 24 h.

After a 3-day incubation, when the primary root of both Ji1037 and HZ4 had grown to 3–5 cm in length, artificial inoculation was performed. Compatible *S. reilianum* colonies were individually inoculated into 200 mL of PDB, followed by propagation on a rotary shaker at 220 r min^{-1} at 24 °C for

3 days. Spore concentration was estimated with a hemocytometer under a microscope. A 200-mL culture of each colony was centrifuged at 2500 r min^{-1} for 10 min. Spores were rinsed once in water and diluted to 2×10^7 spores mL^{-1} . Spores from compatible *S. reilianum* colonies were mixed to inoculate maize seedlings at 3 days post-germination by dipping the primary roots into the filtered spore suspension.

2.5. Observation of *S. reilianum* hyphae

For each inbred line, the primary roots of three seedlings were harvested at 12, 24, 36, and 48 h post-inoculation (hpi), respectively. Similarly, root–stem junctions of three seedlings were collected at 3 and 6 days post-inoculation (dpi) and cut into slices longitudinally. All samples were then fixed overnight at 4 °C in 2.5% (*v/v*) glutaraldehyde, rinsed with water, incubated in ethanol overnight, washed once with water, and then incubated in 10% (*w/v*) KOH overnight. After rinsing with water, the samples were soaked in a staining solution (phosphate-buffered saline solution [pH 7.4] containing 10 $\mu\text{g mL}^{-1}$ WGA–Alexa Fluor 488, 20 $\mu\text{g mL}^{-1}$ propidium iodide, and 0.02% [*v/v*] Tween 20) at 37 °C for 12 min followed by a 3-min vacuum infiltration. After staining, the samples were observed under a laser scanning confocal microscope (Zeiss). WGA–Alexa Fluor 488 was detected with a 488 nm excitation and 500–540 nm emission wavelength and propidium iodide was detected with a 561 nm excitation and 580–660 nm emission wavelength [20].

2.6. Routine PCR-based diagnosis of *S. reilianum*

Apart from maize seedlings used for sampling in the laboratory, the remaining seedlings at 4 dpi were transferred to a 1:1 (*v/v*) vermiculite/nutrient soil mixture and grown in an incubator under 16-h day/8-h night conditions at 26 °C and 60% relative humidity. After 1 week of incubation, the seedlings were transplanted to the field at the Shangzhuang Experimental Farm, China Agricultural University, Beijing.

To trace the spread of endophytic *S. reilianum*, tissues from both Ji1037 and HZ4 at four growing stages were collected, including the early seedling stage at 9 dpi, the seedling stage (1 month after transplanting in the field), the jointing stage (just prior to heading), and the grain filling stage (3 days after pollination). The tissues sampled were the youngest expanding leaf (at all four stages), basal stem, mid-stem, shoot apex (at the seedling stage, the jointing stage and the grain filling stage), ear, and tassel (at the jointing stage and the grain filling stage), which were individually collected from each of 20 plants. In total, 80 leaf samples, 60 basal stem samples, 60 mid-stem samples, 60 shoot apex samples, 40 ear samples, and 40 tassel samples were harvested for each inbred line. A 0.1 g portion of tissue of each leaf sample was directly ground into powder in liquid nitrogen for DNA extraction. The other tissues were first dehydrated in allochroic silica gel for 3 days and then ground into powder in liquid nitrogen. DNA was isolated following the procedure described by Murray and Thompson [22]. Each DNA sample was evaluated for purity and concentration with a Thermo Scientific NanoDrop 1000 spectrophotometer, and adjusted to a consensus concentration of 100 ng μL^{-1} . DNA samples were

amplified with the *S. reilianum*-specific primer SR1 by conventional PCR [10].

2.7. Real-time PCR method for quantitative assay of *S. reilianum*

The *S. reilianum*-specific primer suitable for real-time PCR assay was redesigned based on the sequence of the PCR products amplified with primer SR1. The real-time PCR reaction mixture contained 10 μL SYBR Premix Ex Taq II, 2 μL template DNA, 0.4 μL of each primer (0.01 nmol μL^{-1}), and 7.2 μL ddH₂O in a total volume of 20 μL . The real-time PCR program consisted of an initial denaturation step at 95 °C for 5 min, followed by 40 cycles of 10 s at 95 °C, 15 s at 60 °C, and 30 s at 72 °C, and then was terminated by melting.

For quantitative assay of *S. reilianum* by real-time PCR, a standard curve was first constructed to estimate *S. reilianum* concentration in tissues of inoculated plants. *S. reilianum* DNA (10 ng μL^{-1} , measured with a Thermo Scientific NanoDrop 1000 spectrophotometer) was diluted to five concentrations: 1, 10^{-1} , 10^{-2} , 10^{-3} , or 10^{-4} ng μL^{-1} with 100 ng μL^{-1} HZ4 DNA to set up gradient ratios of *S. reilianum* DNA to maize genomic DNA as templates for real-time PCR. A standard curve and

correlation equation were established for the concentration of *S. reilianum* DNA and corresponding CT values using the software Rotor-Gene Q Series [24].

All samples from the above routine PCR-based diagnosis were subjected to the newly developed real-time PCR to estimate *S. reilianum* content. Each DNA sample was repeatedly assayed three times and the CT value was converted to the concentration of *S. reilianum* DNA based on the correlation equation. The mean concentration of *S. reilianum* DNA and standard deviation (SD) were calculated for 20 samples of each tissue. A one-way ANOVA was fitted to test the statistical significance of differences in hyphal content between Ji1037 and HZ4.

3. Results

3.1. Purification and identification of *S. reilianum*

For every colony culture, four spore types were observed, including spindle-shaped spores, budding spores, spores forming conjugation tube, and fusing compatible spores (Fig. 1A). After amplification with the *S. reilianum*-specific primer

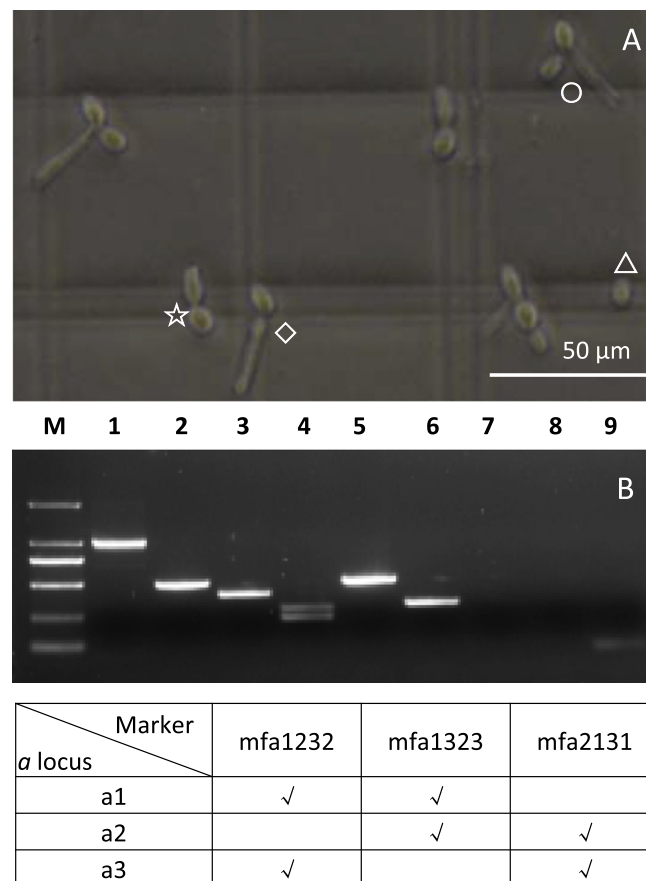


Fig. 1 – Examination of spore types and identification of mating types of *S. reilianum*. **A:** Four spore types in the *S. reilianum* culture: spindle-shaped spores (Δ), budding spores (\star), spores forming conjugation tube (\diamond), and fusing compatible spores (\circ). **B:** Amplification of genomic DNA from a single *S. reilianum* colony with a series of primer pairs. Lanes 1–9: *S. reilianum*-specific marker SR1 (1), *S. reilianum* *a* loci-specific markers mfa1232 (2), mfa1323 (3), mfa2131 (4), and *S. reilianum* *b* loci-specific markers bw1 (5), bw2 (6), bw3 (7), bw4 (8), and bw5 (9). PCR products were observed for the markers SR1 (1), mfa1232 (2), mfa1323 (3), mfa2131 (4), bw1 (5), and bw2 (6), but not for bw3 (7), bw4 (8), and bw5 (9). M, DNA ladder DM2000 (2000, 1000, 750, 500, 200, and 100 bp).

Table 1 – List of *S. reilianum* mating locus-specific markers and *S. reilianum*-specific real-time PCR markers.

Marker name	Primer sequence (5'-3')	Product size (bp)
mfa1232	F: GATCTCGGATTAGGCCATGA; R: CGAACACCAATCCAACACTG	466
mfa1323	F: TGAGTGTGGTTCGTCTCCAG; R: GGAATTGAGCCCAAAGAATG	381
mfa2131	F: GCCTCTGTCCAGGCTGTTT; R: CAACCCATCTGCAAAGGAAC	234
bw1	F: CCCTTGCGGTCTTCGTGT; R: GACCCAGACCTCTGATTCACCT	487
bw2	F: ACTGCTGCTACTGTATCGA; R: AAGTCTCATCGGGTTGCC	309
bw3	F: CAGCGACCGCTATTCCTA; R: AATGATGTCCACAGTCTCC	379
bw4	F: CTTGATGATGTGTCGGTTG; R: CAGTCCTATCCACGCTGAG	446
bw5	F: TCGACTGGTCTTCGATGATG; R: CGGATTCTGCTTCAACTTCA	493
SR161	F: TCTTTCCCGCTCCAAGAAGT; R: CGTGAACCGATGGAGAAAGT	159

F: forward; R: reverse.

pair SR1, a 960 bp PCR product was observed for each of the twenty colonies (Fig. 1B), which had a sequence identical to that of *S. reilianum* by BLAST at NCBI. In addition, the mating type-specific primer pairs (mfa1232, mfa1323, mfa2131, and bw1–bw5) were used to amplify each *S. reilianum* colony, and PCR bands were observed for mfa1232, mfa1323, mfa2131, bw1, and bw2, but not for bw3, bw4, and bw5 (Table 1 and Fig. 1B). *S. reilianum* colonies that showed PCR bands of any two of the three a-locus markers carried one *a* allele, and colonies that showed PCR bands of all three a-locus markers carried at least two *a* alleles (Fig. 1B). Given that all colonies shared the same banding pattern with all PCR products for all three a-locus markers, they contained at least two compatible mating types and thus were eligible for use in inoculating the maize seedlings.

3.2. Performance of *S. reilianum* in early-root infection

Artificial inoculation was performed at 3 days after germination, when the primary root had grown to 3–5 cm for both the Ji1037 and HZ4 inbred lines (Fig. 2A). Substantial numbers of *S. reilianum* hyphae were observed at the root surfaces of both Ji1037 and HZ4 at 12 hpi (Fig. 2B). Thereafter, large numbers of *S. reilianum* hyphae on the root surface were consistently present at 24, 36, and 48 hpi for both Ji1037 and HZ4. At 3 dpi, no *S. reilianum* hyphae were detected in the root–stem junctions for either Ji1037 or HZ4. At 6 dpi, however, *S. reilianum* hyphae were observed in the root–stem junctions of both Ji1037 and HZ4 (Fig. 2C).

3.3. PCR-based detection of *S. reilianum*

The genomic DNA extracted from the youngest expanding leaves at 9 dpi was amplified using the *S. reilianum*-specific SR1 primer, and PCR products were observed in 5 of 20 Ji1037 plants and 6 of 20 HZ4 plants (Table 2). At the seedling stage, *S. reilianum* DNA was not detected in any of the collected tissues

from 20 Ji1037 plants inoculated with *S. reilianum* (Table 2). In contrast, 14 of the 20 inoculated HZ4 plants contained *S. reilianum* DNA in one or multiple tissues (Table 2). At the jointing stage, 6 of 20 inoculated Ji1037 plants contained *S. reilianum* DNA in the youngest expanding leaves. By contrast, 16 of 20 inoculated HZ4 plants contained *S. reilianum* DNA in various tissues (Table 2). At the grain filling stage, *S. reilianum* DNA was detected in 7 of 20 inoculated Ji1037 plants and 18 of 20 inoculated HZ4 plants. The infected tissues of Ji1037 were concentrated in the youngest leaves, lower shoot region, and roots of plants, whereas the infected tissues of HZ4 were found throughout the plant including the ear and tassel (Table 2).

3.4. Establishment of a real-time PCR method for quantitative detection of *S. reilianum*

The PCR method described above can detect only the presence or absence of *S. reilianum* and not the quantity of pathogen present in infected tissues. To monitor infection severity, we need a quantitative method to estimate the quantity of *S. reilianum* in different tissues.

We sequenced the PCR products amplified with the *S. reilianum*-specific primer SR1 and compared those sequences with the *S. reilianum* genomic DNA deposited in NCBI. Interestingly, the SR1 marker sequence exactly matched the *S. reilianum* mitochondrial DNA (accession: FQ311469.1). Based on this piece of the mitochondrial DNA, we used Primer3 to design 10 primer pairs, each of which was designed to generate a PCR product of 150–200 bp. All primer pairs were used to perform routine PCR using template DNAs extracted from Ji1037, HZ4, infected Ji1037 and HZ4 leaf tissues, and *S. reilianum* genomic DNA. The *S. reilianum*-specific primer pairs that produced distinct and uniform PCR products for the *S. reilianum* and infected Ji1037 and HZ4 DNA templates were expected to perform well in real-time PCR analysis. Of these primer pairs, SR161 was one of the best choices (Table 1). Using routine PCR, SR161 could easily amplify *S. reilianum*, but not maize genomic DNA. Using real-time PCR, SR161 produced two non-specific weak peaks in the melting curves for maize DNA (Fig. 3A). There was one distinct *S. reilianum* peak in the melting curves of both infected maize tissues and *S. reilianum* (Fig. 3A).

To estimate the *S. reilianum* concentration in the infected maize tissues, a standard curve was constructed. *S. reilianum* DNA samples with gradient concentrations of 1, 10⁻¹, 10⁻², 10⁻³, and 10⁻⁴ ng μL⁻¹ in 100 ng μL⁻¹ HZ4 DNA were subjected to real-time PCR. The resulting CT values perfectly matched the concentrations of *S. reilianum* DNA. A standard curve and correlation equation were established for the concentrations of *S. reilianum* DNA and corresponding CT values using Rotor-Gene Q Series (Fig. 3B). The standard equation ($R^2 = 0.99$) was as follows:

$$\text{Concentration of } S. reilianum \text{ DNA} = 10^{(-0.307CT+4.100)}, (10 \leq CT \leq 25).$$

3.5. Estimation of pathogen levels in maize tissues by real-time PCR

Individual total genomic DNA samples from various tissues of inoculated maize plants that were collected at 9 dpi and

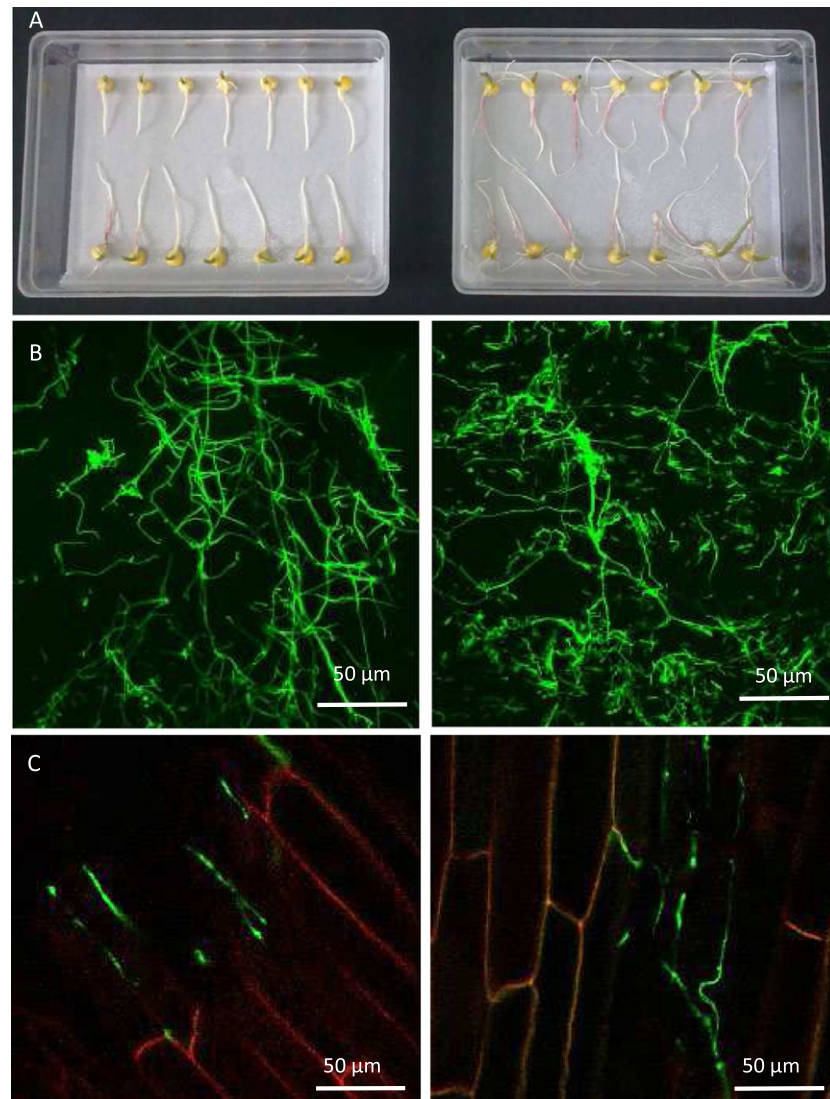


Fig. 2 – Detection of *S. reilianum* hyphae in early-root invasion. A: Three-day-old seedlings of Ji1037 (left) and HZ4 (right) on which *S. reilianum* was artificially inoculated. **B:** *S. reilianum* hyphae were observed on the root surface of Ji1037 (left) and HZ4 (right) at 12 h post-inoculation using a laser scanning confocal microscope (green, fungal hyphae). **C:** *S. reilianum* hyphae were found in the root–stem junction regions of Ji1037 (left) and HZ4 (right) at 6 days post-inoculation (green, fungal hyphae; red, plant cells).

seedling, jointing, and grain filling stages were first adjusted to $100 \text{ ng } \mu\text{L}^{-1}$ and then used as templates for real-time PCR with SR161. The resulting CT values were converted to *S. reilianum* DNA concentrations based on the standard equation. At 9 dpi, *S. reilianum* DNA concentrations were at low levels in the youngest expanding leaf tissues, but there was no significant difference between Ji1037 and HZ4 plants (Fig. 4A). At the seedling stage, *S. reilianum* DNA was not detected in any tissues collected from the inoculated Ji1037, whereas small amounts of *S. reilianum* DNA were detected in the basal stems, mid-stems, shoot apices, and leaves collected from the inoculated HZ4 (Fig. 4B). At the jointing stage, *S. reilianum* DNA was detected only at low levels in the leaves of the inoculated Ji1037 but was detected at varying concentrations in all tissues collected from the inoculated HZ4 (Fig. 4C). At the grain filling stage, *S. reilianum* DNA was detected at low levels in the leaves, basal stems, mid-stems, and shoot apices

of the inoculated Ji1037, whereas large amounts were detected in all regions (except leaves) of the inoculated HZ4 (Fig. 4D). Disease incidence was investigated in the remaining plants at maturity. None of the Ji1037 plants showed disease symptoms, whereas HZ4 showed ~80% disease incidence.

4. Discussion

4.1. Methods for plant pathogen detection

Soilborne *S. reilianum* invades maize roots at the seedling stage [2], and grows upwards endophytically. When the *S. reilianum* hyphae reach either ear or tassel of maize, they may switch from biotrophic to necrotrophic growth and cause disease symptoms. Our results showed that, in most cases, plants infected by *S. reilianum* fail to show symptoms because

Table 2 – Number of tissues infected by *S. reilianum* in inoculated Ji1037 and HZ4 plants.

Harvesting stage	Inbred line	Total number of infected plants ^a	Infected leaves	Infected basal stems	Infected mid-stems	Infected shoot apices	Infected ears	Infected tassels
Early seedling stage	Ji1037	5	5	/	/	/	/	/
	HZ4	6	6	/	/	/	/	/
Seedling stage	Ji1037	0	0	0	0	0	/	/
	HZ4	14	6	11	5	5	/	/
Jointing stage	Ji1037	6	6	0	0	0	0	0
	HZ4	16	6	13	12	7	4	3
Grain filling stage	Ji1037	7	5	6	4	2	0	0
	HZ4	18	11	18	17	14	12	10

The four developmental stages include: 1) early seedling stage at 9 dpi, 2) seedling stage (1 month after transplanting in the field), 3) jointing stage (just prior to heading), and 4) grain filling stage (3 days after pollination)

/No sample available.

^a A plant was defined as infected if at least one of the collected tissues was detected to contain *S. reilianum* via PCR-based diagnosis. In total 20 samples were tested for every tissue at each developmental stage for both Ji1037 and HZ4.

of retarded hyphal growth. For this reason, pre-diagnosis of infected plants is of importance for predicting disease severity and distinguishing resistant from susceptible maize varieties. To date, several methods have been developed to detect *S. reilianum*, including hyphal staining [20], PCR detection [10],

and real-time PCR analysis. Hyphal staining can visually reveal the growth of the pathogen. During early-root infection, root surfaces and root-stem junction regions are the optimal regions for hyphal staining and observation. However, as the maize plants develop, more tissues and organs need

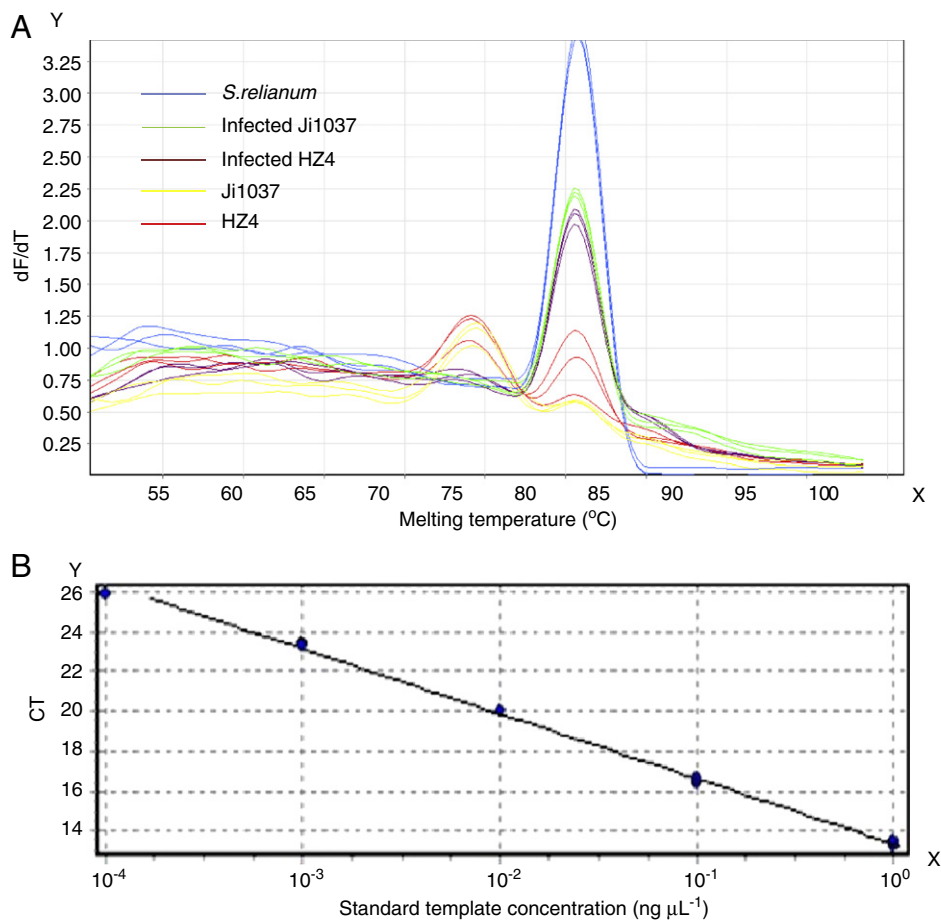


Fig. 3 – Real-time PCR method for quantitative detection of *S. reilianum*. A: Melting curves for real-time PCR marker SR161 using genomic DNA from uninfected and infected maize and *S. reilianum*. X axis, melting temperature; y axis, abundance of PCR product. B: Standard curve generated based on the template concentration and corresponding CT value using the software Rotor-Gene Q Series. CT values ranging from 10 to 25 were used for prediction of pathogen concentration.

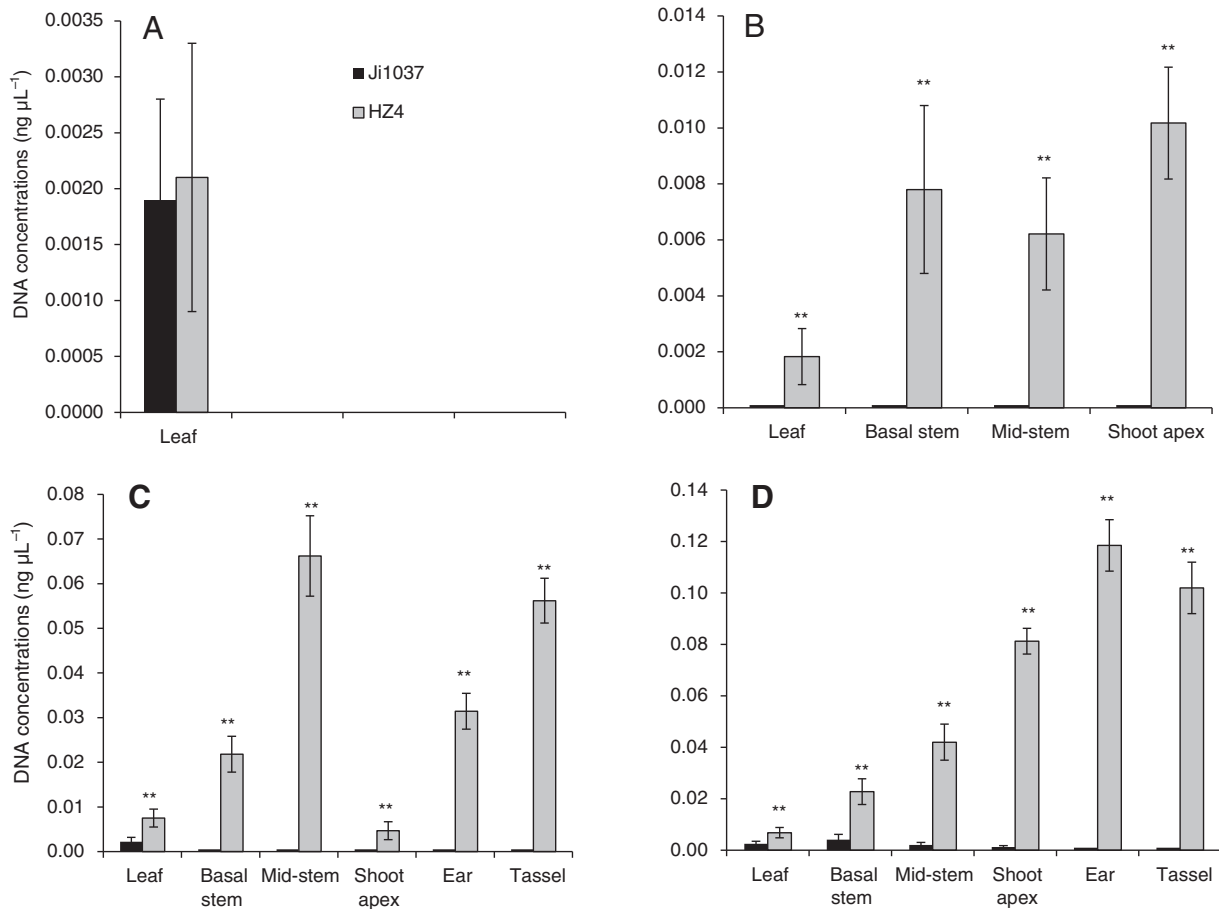


Fig. 4 – Quantitative detection of *S. reilianum* DNA concentrations (ng µL⁻¹) based on real-time PCR. A: Early seedling stage at 9 dpi. B: Seedling stage (1 month after transplanting to the field). C: Jointing stage (just prior to heading). D: Grain filling stage (3 days after pollination). ** Significant difference between the two inbred lines at $P = 0.01$.

to be tested because of the unpredictable growth of the pathogen. In this situation, hyphal staining is too expensive and time-consuming to use for surveying large numbers of samples. PCR-based detection of the pathogen would be a fast and cost-effective way to solve this problem. However, classical PCR is capable of determining only the presence or absence of the pathogen in plant tissue and not the quantity of pathogen, which is also important for research. The real-time PCR method described here allows quantitative detection in *S. reilianum* in infected tissues for monitoring the process of hyphal growth.

The availability of the *S. reilianum* genome sequence facilitates the design of optimal primers for both PCR and real-time PCR [25]. The *S. reilianum*-specific marker SR1 was derived from mitochondrial DNA, according to our NCBI BLAST results comparing the *S. reilianum* PCR product and genomic sequences. The multiple copies of this sequence in mitochondrial DNA likely represent *S. reilianum*-specific repetitive DNA sequences from which suitable PCR primers can be designed for sensitive, specific PCR amplification. In view of the large SR1 PCR product size (960 bp), we designed new primers within this region to shorten the PCR products for real-time PCR. After several rounds of selection, we determined that marker SR161 had sensitivity equal to that of SR1, which could quantitatively detect up to 1×10^{-4} ng µL⁻¹

S. reilianum DNA by real-time PCR. We also designed several primer pairs for discrimination of the mating loci. Although these markers are capable of identifying the mating types for different purified pathogen clones, they could not be used to identify the pathogen levels in the infected maize tissues because of their relatively low sensitivity.

4.2. Mechanism underlying resistance to head smut in maize

Unlike *U. maydis* infection, which can rapidly lead to the generation of prominent tumor-like structures on all vegetative and reproductive regions of maize [26], *S. reilianum* produces less visible symptoms on these vegetative organs [27]. After infection, *S. reilianum* grows in the form of dikaryotic parasitic hyphae inside maize until the occurrence of fungal sporulation in the floral organs [18]. The observation that *S. reilianum* sporulates only in floral structures leads to two alternative hypotheses: (1) dikaryotic parasitic hyphae reach the floral organs only in susceptible and not resistant maize plants; (2) dikaryotic parasitic hyphae can reach the floral organs of both resistant and susceptible maize plants, but fungal sporulation occurs only in susceptible plants.

In the first hypothesis, we needed to identify the difference between resistant and susceptible plants during initial pathogen invasion and subsequent pathogen growth. We found

no difference between resistant Ji1037 and susceptible HZ4 with respect to *S. reilianum* germination at the root surface (Fig. 2B), penetration of root epidermal cells, or initial growth from the roots toward the root-stem junction (Fig. 2C). This result was in agreement with previous expression profiles showing few significantly differentially expressed genes between the resistant Mo17 and susceptible HZ4 inbred lines before the eighth-leaf stage [21]. In contrast, marked differences in pathogen spread were observed. No pathogen (Ji1037) and a substantial mass of pathogen (HZ4) were detected in the floral organs of inoculated plants (Fig. 4C and D). In the field survey, Ji1037 showed no disease incidence, whereas ~80% of the HZ4 plants showed prominent sori in either their ears or tassels.

In summary, the resistance to head smut in Ji1037 was associated mainly with suppression of pathogen spread and not with resistance to pathogen penetration. The low amount or absence of *S. reilianum* hyphae in the floral organs renders it less likely to cause symptoms in the resistant line Ji1037.

Acknowledgments

This work was funded by the Ministry of Agriculture of China (2013ZX08009003-001-007), and the National High Technology Research and Development Program of China (2012AA101104, 2012AA10A306).

REFERENCES

- [1] T. Lübberstedt, X.C. Xia, G.Q. Tan, X. Liu, A.E. Melchinger, QTL mapping of resistance to *Sporisorium reilianum* in maize, *Theor. Appl. Genet.* 99 (1999) 593–598.
- [2] R.A. Frederiksen, Head smuts of corn and sorghum, *Proc. Corn Sorghum Res. Conf.* 32 (1977) 89–104.
- [3] S. Zhang, Y. Xiao, J. Zhao, F. Wang, Y. Zheng, Digital gene expression analysis of early root infection resistance to *Sporisorium reilianum* f. sp. *zeae* in maize, *Mol. Genet. Genomics* 288 (2013) 21–37.
- [4] C. Martinez, A. Jauneau, C. Roux, C. Savy, R. Dargent, Early infection of maize roots by *Sporisorium reilianum* f. sp. *zeae*, *Protoplasma* 213 (2000) 83–92.
- [5] C.T. Ingold, Products of teliospore germination in *Sporisorium* spp., *Mycol. Res.* 98 (1994) 467–473.
- [6] W.F. Hanna, Studies in the physiology and cytology of *Ustilago zeae* and *Sorosporium reilianum*, *Phytopathology* 19 (1929) 415–442.
- [7] C. Martinez, C. Roux, A. Jauneau, R. Dargent, The biological cycle of *Sporisorium reilianum* f. sp. *zeae*: an overview using microscopy, *Mycologia* 94 (2002) 505–514.
- [8] J. Schirawski, B. Heinze, M. Wagenknecht, R. Kahmann, Mating type loci of *Sporisorium reilianum*: novel pattern with three a and multiple b specificities, *Eukaryot. Cell* 4 (2005) 1317–1327.
- [9] N. Capote, A.M. Pastrana, A. Aguado, P. Sánchez-Torres, Molecular tools for detection of plant pathogenic fungi and fungicide resistance, *Plant Pathol.* (2012) 151–202.
- [10] M.L. Xu, A.E. Melchinger, T. Lübberstedt, Species-specific detection of the maize pathogens *Sporisorium reilianum* and *Ustilago maydis* by dot blot hybridization and PCR-based assays, *Plant Dis.* 83 (1999) 390–395.
- [11] G.Q. Tan, Y.X. Xing, M.L. Xu, Z. Cai, Discovery and verification about the phenomena of germ-carrying plant with head smut of maize, *J. Maize Sci.* 3 (2009) 120–122.
- [12] S. Ni, Y.N. Xiao, F.G. Wang, J.R. Zhao, S.P. Zhang, Y.L. Zheng, The research of *Sporisorium reilianum*'s infection efficiency and spreading in maize based on PCR assays, *Sci. Agric. Sin.* 39 (2005) 1804–1809.
- [13] Y.M. Shi, D.Y. Li, Study on the characteristic of *Sporisorium reilianum* spores using Fourier transform infrared spectroscopy, *Photonics Optoelectronics (SOPO)* 2012. 1–3.
- [14] Z.D. He, C. Jie, Z.G. Gao, J.H. Zhang, Progress on studies of head smut physiological differential in maize, *J. Maize Sci.* 13 (2005) 117–120.
- [15] W.L. Zuo, Q. Chao, N. Zhang, J.R. Ye, G.Q. Tan, B.L. Li, Y.X. Xing, B.Q. Zhang, H.J. Liu, K.A. Fengler, J. Zhao, X.R. Zhao, Y.S. Chen, J.S. Lai, J.B. Yan, M.L. Xu, A maize wall-associated kinase confers quantitative resistance to head smut, *Nat. Genet.* 47 (2015) 151–157.
- [16] Y.S. Chen, Q. Chao, G.Q. Tan, J. Zhao, M.J. Zhang, Q. Ji, M.L. Xu, Identification and fine-mapping of a major QTL conferring resistance against head smut in maize, *Theor. Appl. Genet.* 117 (2008) 1241–1252.
- [17] X.R. Zhao, G.Q. Tan, Y.X. Xing, L. Wei, Q. Chao, W.L. Zuo, T. Lübberstedt, M.L. Xu, Marker-assisted introgression of *qHSR1* to improve maize resistance to head smut, *Mol. Breed.* 30 (2012) 1077–1088.
- [18] C.A. Matyac, Histological development of *Sphacelotheca reilianum* on *Zea mays*, *Phytopathology* 75 (1985) 924–929.
- [19] C. Martinez, C. Roux, R. Dargent, Biotrophic development of *Sporisorium reilianum* f. sp. *zeae* in vegetative shoot apex of maize, *Phytopathology* 89 (1999) 247–253.
- [20] H. Ghareeb, A. Becker, T. Iven, I. Feussner, J. Schirawski, *Sporisorium reilianum* infection changes inflorescence and branching architectures of maize, *Plant Physiol.* 156 (2011) 2037–2052.
- [21] S. Zhang, J. Gardiner, Y. Xiao, J. Zhao, F. Wang, Y. Zheng, Floral transition in maize infected with *Sporisorium reilianum* disrupts compatibility with this biotrophic fungal pathogen, *Planta* 237 (2013) 1251–1266.
- [22] M.G. Murray, W.F. Thompson, Rapid isolation of high molecular-weight plant DNA, *Nucleic Acids Res.* 8 (1980) 4321–4325.
- [23] M.A. Larkin, G. Blackshields, N.P. Brown, Clustal W and Clustal X version 2.0, *Bioinformatics* 23 (21) (2007) 2947–2948.
- [24] Y. Dai, W. Sui, H. Lan, Q. Yan, H. Huang, Comprehensive analysis of microRNA expression patterns in renal biopsies of lupus nephritis patients, *Rheumatol. Int.* 29 (2009) 749–754.
- [25] N.W. Schaad, R.D. Frederick, Real-time PCR and its application for rapid plant disease diagnostics, *Can. J. Plant Pathol.* 24 (2002) 250–258.
- [26] C.F. Lopez, S. Romero, Factors affecting the development of the Common Corn Smut (Huitlacoche) caused by *Ustilago Maydis* (Dc) Cda, *Phytopathology* 73 (1983) 123–123.
- [27] C.A. Matyac, T. Kommedahl, Occurrence of chlorotic spots on corn seedlings infected with *Sphacelotheca reilianum* and their use in evaluation of head smut resistance, *Plant Dis.* 69 (1985) 251–254.